Disparities in particulate matter (PM_{10}) origins and oxidative potential at a city-scale (Grenoble, France) - Part II: Sources of PM_{10} oxidative potential using multiple linear regression analysis and the predictive applicability of multilayer perceptron neural network analysis

Supplementary information

Table of Contents:

S1. PM characterization

Table S1. Annual average of PM_{10} mass concentrations and chemical compositions (in µg m^{-3}) at all sites, and individual urban sites in Grenoble, France.

Species	All sites	Urban hyper-center (UH)	Urban background (UB)	Peri-urban (PU)
		µg m^{-3}		
PM_{10}	14.4 ± 9.0	16.0 ± 9.6	14.2 ± 8.3	13.1 ± 8.9
OC*	3.89 ± 2.14	4.09 ± 2.11	3.89 ± 2.03	3.7 ± 2.26
EC	1.01 ± 0.84	1.18 ± 0.89	1.12 ± 0.95	0.73 ± 0.58
Cl^-	0.12 ± 0.23	0.16 ± 0.28	0.08 ± 0.14	0.1 ± 0.23
NO_3^-	2.02 ± 2.85	2.55 ± 3.24	1.79 ± 2.53	1.72 ± 2.67
SO_4^{2-}	1.48 ± 1.01	1.58 ± 1.05	1.53 ± 1.02	1.33 ± 0.96
Na^+	0.17 ± 0.18	0.2 ± 0.22	0.15 ± 0.13	0.15 ± 0.18
NH_4^-	0.85 ± 1.05	0.99 ± 1.18	0.81 ± 0.99	0.75 ± 0.98
K^+	0.15 ± 0.12	0.16 ± 0.12	0.15 ± 0.12	0.13 ± 0.11
Mg^{2+}	0.02 ± 0.01	0.02 ± 0.02	0.02 ± 0.01	0.02 ± 0.01
Ca^{2+}	0.32 ± 0.26	0.36 ± 0.28	0.31 ± 0.26	0.3 ± 0.24
MSA	0.02 ± 0.03	0.03 ± 0.03	0.02 ± 0.03	0.02 ± 0.02
Levoglucosan	0.3 ± 0.39	0.25 ± 0.31	0.28 ± 0.35	0.36 ± 0.49
Mannosan	0.03 ± 0.04	0.03 ± 0.04	0.03 ± 0.04	0.04 ± 0.05
Polyols	0.04 ± 0.04	0.04 ± 0.04	0.04 ± 0.04	0.05 ± 0.05
Cellulose	0.08 ± 0.08	0.13 ± 0.09	0.05 ± 0.04	0.06 ± 0.07
		ng m^{-3}		
3-MBTCA	9.13 ± 9.72	9.8 ± 10.08	8.5 ± 9.21	9.09 ± 9.89
Phthalic acid	3.54 ± 3.48	3.5 ± 2.92	3.88 ± 4.63	3.24 ± 2.52
Pinic acid	6.61 ± 7.19	5.36 ± 5.79	5.25 ± 4.37	9.22 ± 9.64
Al	0.06 ± 0.09	0.06 ± 0.08	0.07 ± 0.09	0.06 ± 0.11
As	0.33 ± 0.32	0.41 ± 0.4	0.37 ± 0.31	0.23 ± 0.2
Cd	1.56 ± 2.21	2.2 ± 3.04	1.61 ± 1.8	0.86 ± 1.13
Cr	0.07 ± 0.08	0.08 ± 0.1	0.07 ± 0.08	0.05 ± 0.05
Cu	8.5 ± 7.95	11.59 ± 10.27	8.79 ± 7.24	5.09 ± 3.26
Fe	0.22 ± 0.19	0.24 ± 0.21	0.25 ± 0.2	0.16 ± 0.14
Mn	9.0 ± 14.13	11.73 ± 14.21	7.19 ± 8.08	8.03 ± 17.93
Mo	0.59 ± 0.86	0.8 ± 1.1	0.63 ± 0.89	0.35 ± 0.38
Ni	0.91 ± 0.86	1.18 ± 1.13	0.92 ± 0.74	0.63 ± 0.5
Pb	4.42 ± 5.29	5.73 ± 6.21	4.84 ± 5.64	2.69 ± 2.98
Rb	0.45 ± 0.36	0.48 ± 0.37	0.44 ± 0.34	0.41 ± 0.37
Sb	1.31 ± 4.31	1.71 ± 4.53	1.53 ± 4.83	0.69 ± 3.42
Se	0.39 ± 0.23	0.43 ± 0.23	0.41 ± 0.24	0.32 ± 0.21
Sn	2.26 ± 1.34	2.6 ± 1.48	2.45 ± 1.44	1.73 ± 0.87
Ti	3.81 ± 3.33	4.11 ± 3.26	3.83 ± 3.29	3.49 ± 3.43
V	0.48 ± 0.55	0.51 ± 0.53	0.52 ± 0.57	0.42 ± 0.55

Zn	20.25 ± 29.38	26.1 ± 33.25	23.58 ± 34.26	11.04 ± 13.89

S2. Positive Matrix Factorization (PMF)

Table S2. Summary of tracers used to identify the PM_{10} sources in the PMF analysis.

Identified factors	Specific tracers
Biomass burning	OC*, levoglucosan, mannosan, K^+, Rb, Cl^-
Primary traffic	EC, Ca^{2+}, Cu, Fe, Sb, Sn
Nitrate-rich	NO_3^-, NH_4^+
Sulfate-rich	SO_4^{2-}, NH_4^+, Se
Mineral dust	Ca^{2+}, Al, Ti, V
Sea/road salt	Na^+, Cl^-
Aged sea salt	Na^+, Mg^{2+}
Industrial	As, Cd, Cr, Mn, Mo, Ni, Pb, Zn
Primary biogenic	Polyols, cellulose
MSA-rich	MSA
Secondary biogenic oxidation	3-MBTCA, pinic acid

S3. Various artificial neural network (ANN) architectures tested for the multilayer perceptron (MLP) analysis

Table S3. Various tested ANN architectures and their model performance based on root mean square error (RMSE) and Pearson correlation (*r*). Note: Optimal models per site (with the lowest RMSE and highest *r*) are highlighted in bold.

Site	Model	Activation function	Optimization Algorithm	Learning rate	OP_v^{DTT}		OP_v^{AA}		OP_v^{DCFH}	
					RMSE	r	RMSE	r	RMSE	r
Urban background (UB)	MLP1	TanH	Scaled conjugate	N/A	**0.35**	**0.94**	0.37	0.96	0.25	0.97
	MLP2	Sigmoid	Scaled conjugate	N/A	0.36	0.93	0.35	0.97	0.21	0.98
	MLP3	TanH	Gradient descent	0.2	0.40	0.92	0.39	0.96	0.31	0.95
	MLP4	TanH	Gradient descent	0.4	0.36	0.93	**0.32**	**0.97**	**0.19**	**0.98**
	MLP5	TanH	Gradient descent	0.6	0.39	0.92	0.41	0.96	0.29	0.96
	MLP6	Sigmoid	Gradient descent	0.2	0.38	0.93	0.33	0.97	0.21	0.98
	MLP7	Sigmoid	Gradient descent	0.4	0.38	0.93	0.36	0.97	0.22	0.98
	MLP8	Sigmoid	Gradient descent	0.6	0.39	0.92	0.42	0.96	0.26	0.96
Urban hyper-center (UH)	MLP1	TanH	Scaled conjugate	N/A	0.61	0.84	0.57	0.92	0.36	0.92
	MLP2	Sigmoid	Scaled conjugate	N/A	0.61	0.83	0.54	0.93	0.32	0.94
	MLP3	TanH	Gradient descent	0.2	0.58	0.85	0.58	0.92	0.35	0.92
	MLP4	TanH	Gradient descent	0.4	0.58	0.85	0.57	0.92	0.35	0.93
	MLP5	TanH	Gradient descent	0.6	**0.54**	**0.88**	**0.50**	**0.94**	**0.30**	**0.95**
	MLP6	Sigmoid	Gradient descent	0.2	0.56	0.86	0.52	0.93	0.32	0.94
	MLP7	Sigmoid	Gradient descent	0.4	0.60	0.85	0.53	0.93	0.34	0.93
	MLP8	Sigmoid	Gradient descent	0.6	0.62	0.83	0.72	0.87	0.42	0.89
Peri-urban (PU)	MLP1	TanH	Scaled conjugate	N/A	0.74	0.72	0.74	0.94	0.53	0.95
	MLP2	Sigmoid	Scaled conjugate	N/A	**0.62**	**0.75**	**0.42**	**0.97**	0.31	0.96
	MLP3	TanH	Gradient descent	0.2	0.61	0.65	0.61	0.89	0.36	0.90
	MLP4	TanH	Gradient descent	0.4	0.58	0.71	0.44	0.96	**0.33**	**0.96**
	MLP5	TanH	Gradient descent	0.6	0.66	0.73	0.82	0.95	0.51	0.95
	MLP6	Sigmoid	Gradient descent	0.2	0.61	0.73	0.52	0.96	0.32	0.96
	MLP7	Sigmoid	Gradient descent	0.4	0.60	0.71	0.58	0.96	0.39	0.96
	MLP8	Sigmoid	Gradient descent	0.6	0.59	0.72	0.50	0.96	0.34	0.96

S4. Daily distribution of PM_{10} sources and observed OP activity

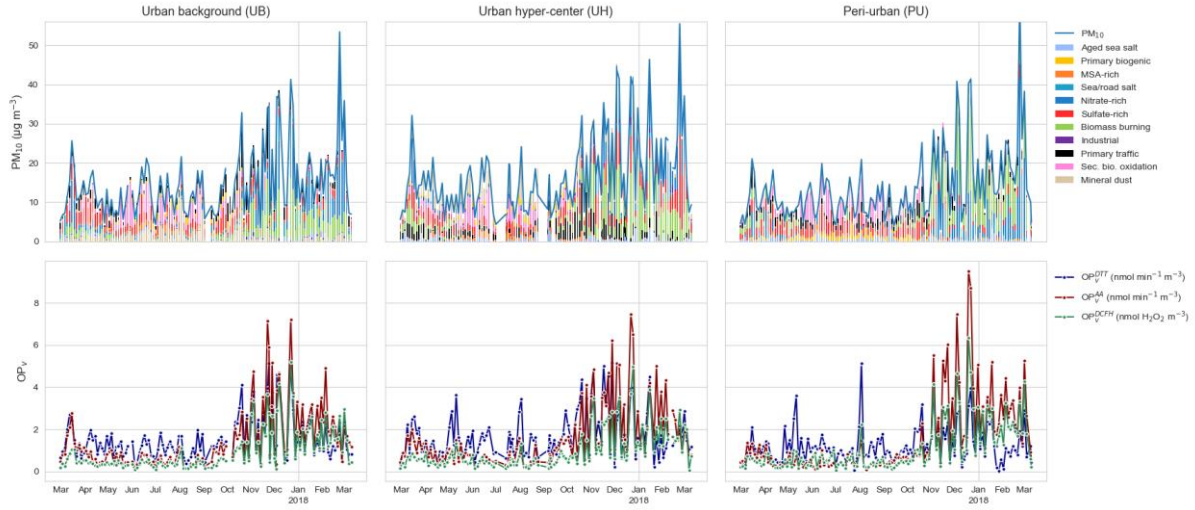

Figure S1: Daily temporal distribution of the reconstructed PM_{10} mass concentration, PMF-resolved sources, and observed OP activity (OP_v^{DTT}, OP_v^{AA}, and OP_v^{DCFH}) in the three urban sites.

S5. Comparison between OP assays

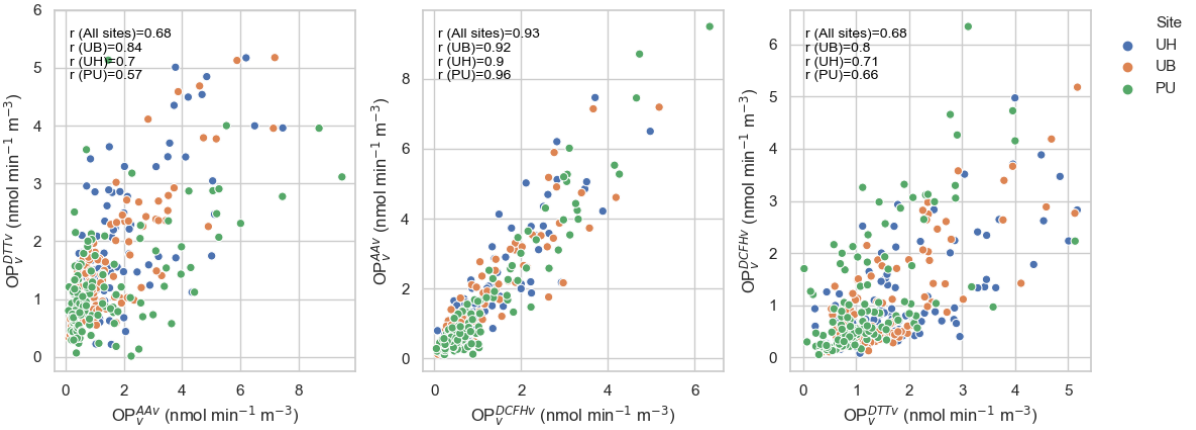

Figure S2: Pair-wise correlation between of the OP assays (left: DTT-AA, center AA-DCFH and right DCFH-DTT). The colors refer to the sampled sites (blue: UH, orange: UB, and green: PU). Pearson *r* coefficient is given for all the sites combined and for individual sites.

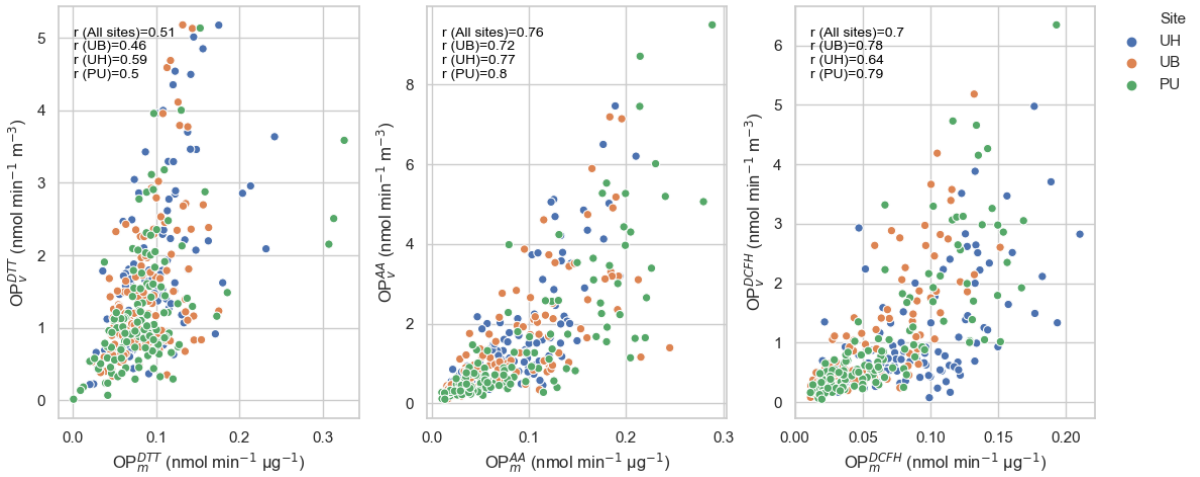

Figure S3: Pair-wise correlation of mass- and volume-normalized OP activity (OP_m and OP_v, respectively) for the three assays (left: DTT, center: AA, and right DCFH). The colors refer to the sampled sites (blue: UH, orange: UB and green: PU). Pearson *r* coefficient is given for all the sites combined and for individual sites.

S6. Comparison of the observed and MLR-modelled OP activity

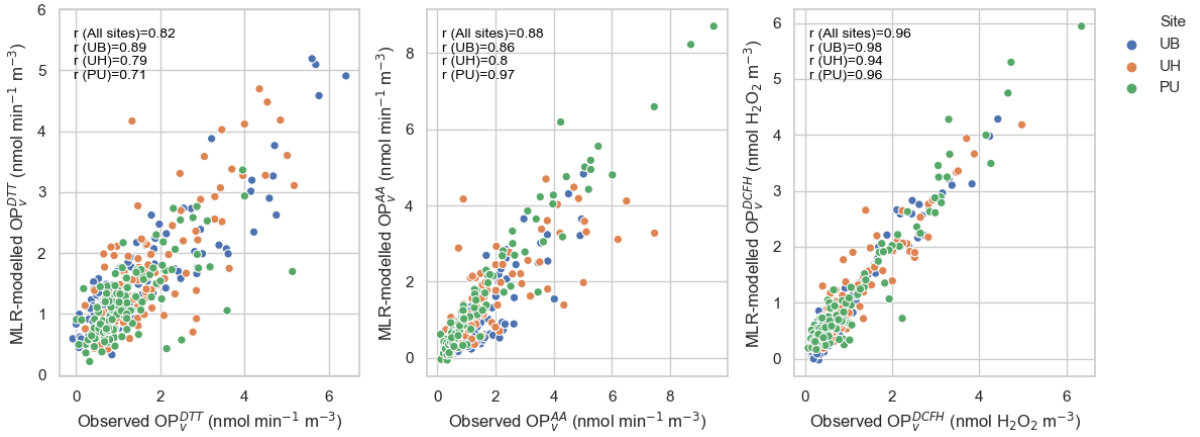

Figure S4: Pair-wise correlation the observed and modelled volume-normalized OP activity for the three assays (left: DTT, center: AA, and right DCFH) using MLR analysis. The colors refer to the sampled sites (blue: UH, orange: UB and green: PU). Pearson *r* coefficient is given for all the sites combined and for individual sites.

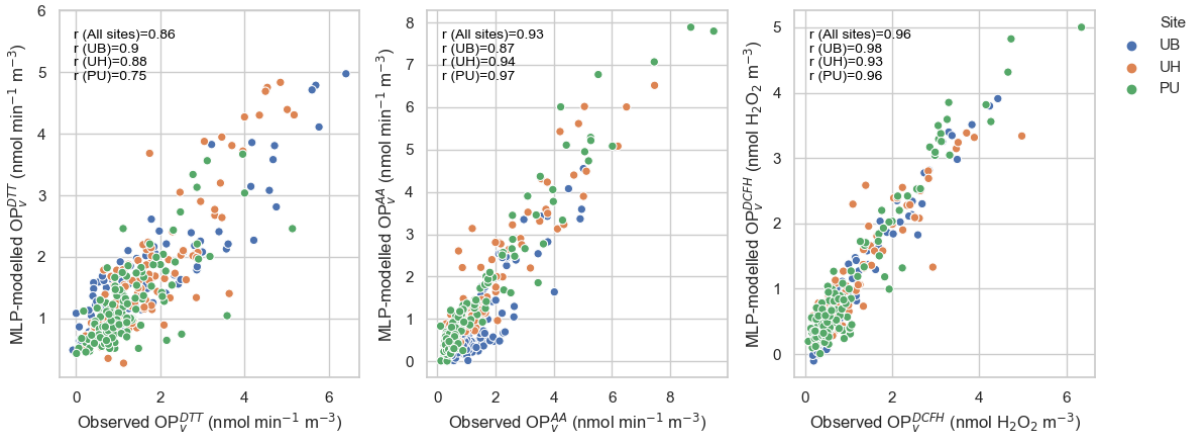

Figure S5: Pair-wise correlation the observed and modelled volume-normalized OP activity for the three assays (left: DTT, center: AA, and right DCFH) using MLP analysis. The colors refer to the sampled sites (blue: UH, orange: UB and green: PU). Pearson *r* coefficient is given for all the sites combined and for individual sites.

S7. Site-specific mean daily contribution of each source to PM_{10} mass and OP activity

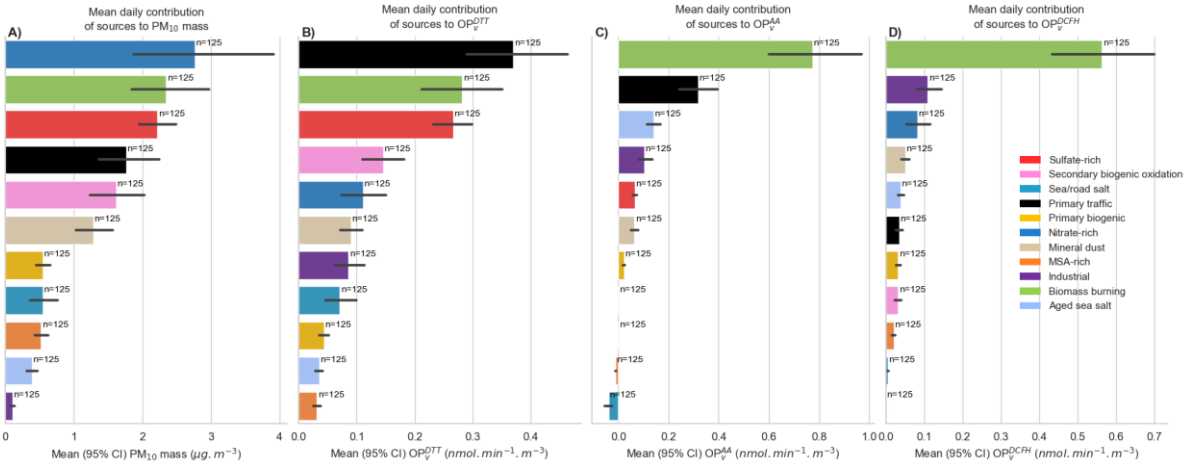

Figure S6: Overall daily mean OP_v contribution of the sources to PM_{10}, OP_v^{DTT}, OP_v^{AA}, and OP_v^{DCFH} using MLR analysis in the UB site in the form of mean and 95% confident interval of the mean (error bar) (n=125 samples).

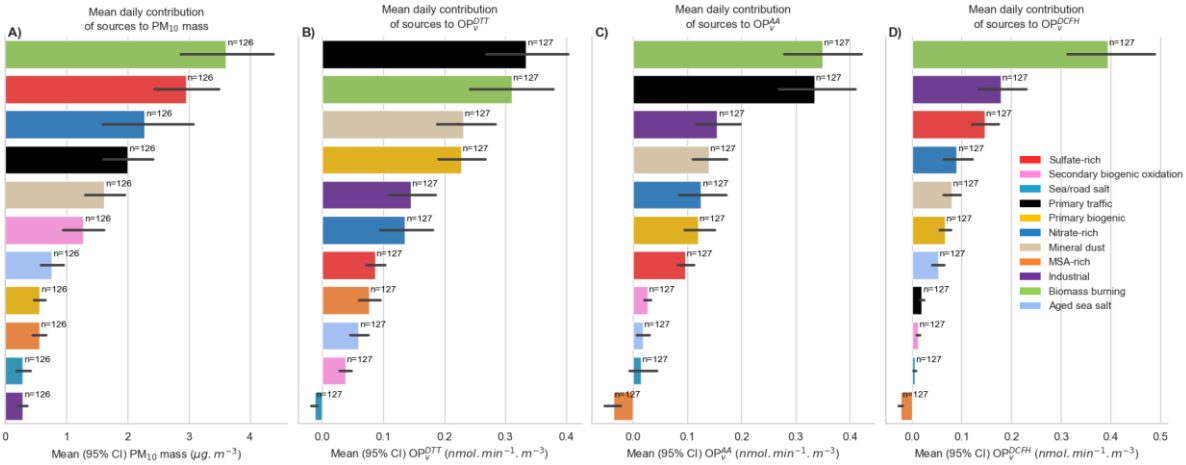

Figure S7: Overall daily mean OP_v contribution of the sources to PM_{10}, OP_v^{DTT}, OP_v^{AA}, and OP_v^{DCFH} using MLR analysis in the UH site in the form of mean and 95% confident interval of the mean (error bar) (n=126 samples).

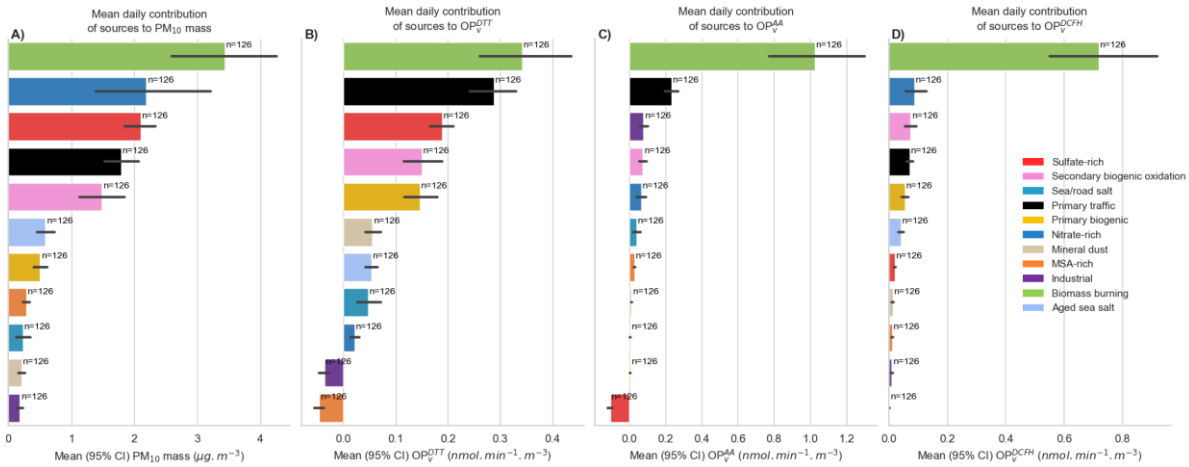

Figure S8: Overall daily mean OP_v contribution of the sources to PM10, OP_v^{DTT}, OP_v^{AA}, and OP_v^{DCFH} using MLR analysis in the PU site in the form of mean and 95% confident interval of the mean (error bar) (n=126 samples).

S8. The non-linearity of OP contributions of PM_{10} sources based on MLP analysis

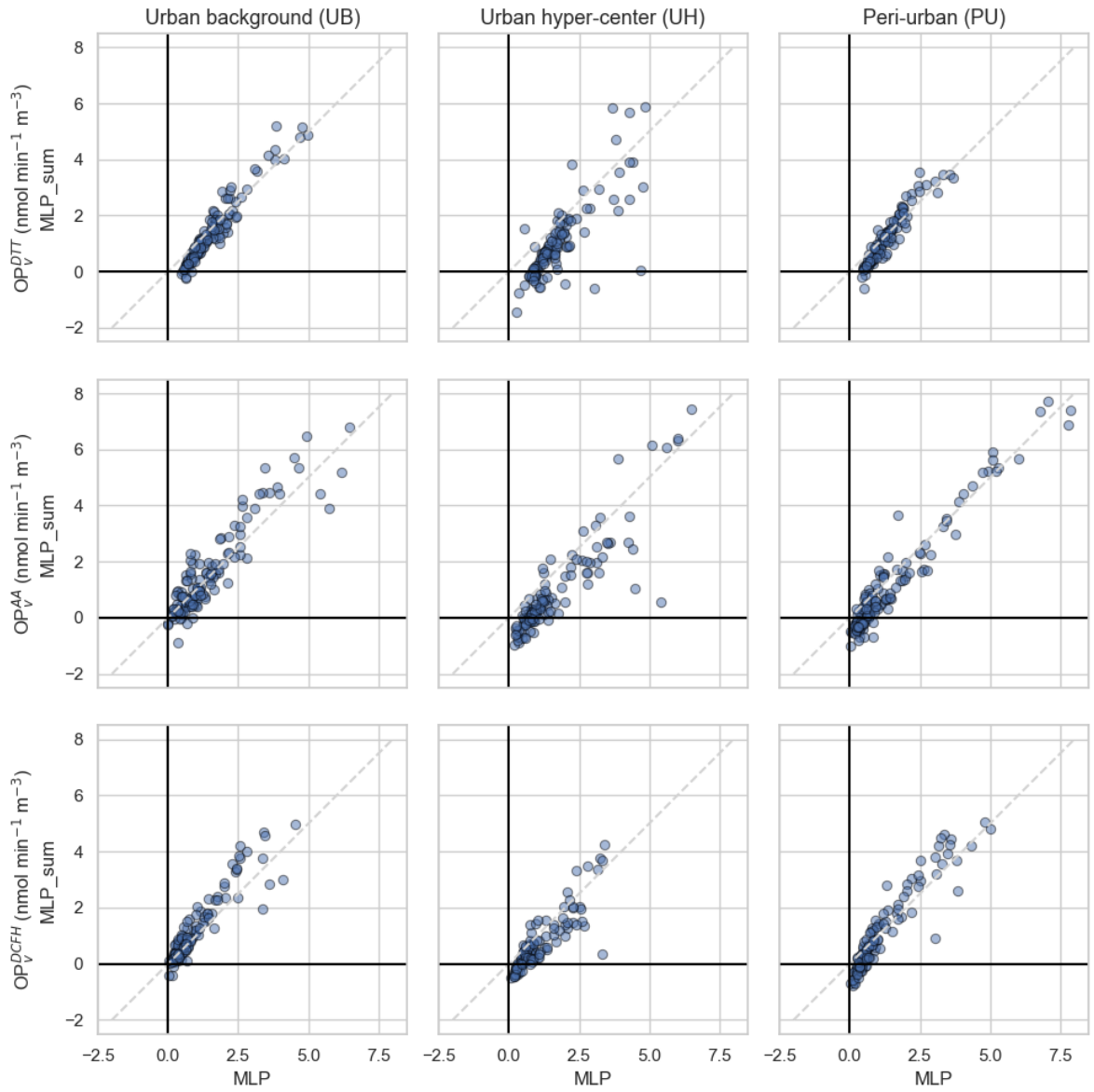

Figure S9: The comparison of the original modelled OP_v (MLP) and the sum of source-specific modelled OP_v activity (MLP_{sum}). Note: Dashed grey line corresponds to the 1:1 line. Data points below the 1:1 shows an over-all synergistic effect between PM_{10} sources on OP activity, above the 1:1 line is otherwise.